J. Fluid Mech. (1985), *vol.* 154, *pp.* 187–213
Printed in Great Britain

The effect of contraction on a homogeneous turbulent shear flow

By K. R. SREENIVASAN
Applied Mechanics, Yale University, New Haven, Connecticut 06520

(Received 8 December 1981 and in revised form 17 May 1984)

A homogeneous turbulent shear flow in its asymptotic stage of development was subjected to an additional (longitudinal) strain by passing the flow through gradual contraction in the direction perpendicular to that of the mean shear. Two contractions, of area ratio 1.4 and 2.6, were used. Mean velocity and turbulent stress (both normal and shear) distributions were measured at several streamwise locations in the contraction region. The mean velocity distributions agree quite well with calculations based on the (inviscid) Bernoulli equation. Until at least half-way down the contraction with the larger area ratio, the rapid-distortion calculations considering only the streamwise acceleration were found to be reasonably successful in predicting the turbulent intensities. For the smaller-area-ratio contraction, corrections for the 'natural development' of the shear flow become important nearly everywhere. Similar calculations considering the shear as the only straining mechanism are generally less successful, although the shear strain rate is at least as rapid as, or even more so than, the longitudinal one. The pressure–rate-of-strain covariance terms estimated from the approximate component energy balance were used to test the adequacy of three models with varying degrees of complexity. Although none of these models appears general enough, their performance is generally adequate for the lower-area-ratio contraction; perhaps not surprisingly, the more complex the model the better its performance.

1. Introduction

The simplest conceivable turbulent shear flow is one in which a homogeneous field of turbulence is maintained by a uniform mean velocity gradient. Such a flow is strictly unattainable experimentally, but several attempts have been made to generate approximations to such an ideal shear flow (Rose 1966; Champagne, Harris & Corrsin 1970; Mulhearn & Luxton 1970, 1975; Harris, Graham & Corrsin 1977; see also Tavoularis & Corrsin 1981). It is now clear that in the earlier experiments of Rose and Champagne *et al.* the flow had not attained its asymptotic state, but Harris *et al.* did succeed in producing a good laboratory approximation to a transversely homogeneous uniformly sheared turbulent flow in its asymptotic state. In this asymptotic state, each of the turbulent energy components grew nearly linearly with the streamwise direction x_1. However, the ratio of any two of them and the shear correlation coefficient,

$$C = -\overline{u_1 u_2}/u_1' u_2', \tag{1}$$

were approximately constant in x_1. Here, u_1 and u_2 are velocity fluctuation components in the x_1- and x_2-directions respectively, x_2 being the direction of mean shear. A prime denotes the root-mean-square value.

The experimental studies mentioned above have served several useful purposes. First, all of them have shed some light on the mechanism of turbulence in the absence of the complex effects of rigid and free boundaries. Secondly, they have served as basic test cases for turbulence modellers, and have provided information useful in the construction of models aimed at even more complex turbulent shear flows (see e.g. Launder, Reece & Rodi 1975; Reynolds 1976, and a host of calculation methods presented in the Stanford meeting on Complex Turbulent Flows, 1981). Also, attempts have been made to simulate these relatively simple flows directly on a computer (Feiereisen *et al.* 1981). As an obvious sequel to the research cited above, it seemed that a study of the effects of additional complexities imposed on the homogeneous shear flow was worthwhile. We elected to impose an extra streamwise strain on the flow in its asymptotic development. The primary purpose of this paper is to document some aspects of such a flow field.

A second purpose of this paper is to evaluate from an approximate component energy balance the turbulent pressure–rate-of-strain covariance terms in the equations for the normal Reynolds stresses. (For brevity we shall designate them simply as pressure–strain terms.) These terms defy simple and direct means of measurement in most laboratory flows, and pose a challenge to turbulence modellers. Nearly all estimates made of these terms have been via turbulent energy balance, but such estimates are not always reliable owing to uncertainties in the measurement of other quantities, especially the triple-correlation terms. Reliable estimates have been made only in relatively simple flows, with the mean strain rate either entirely absent (Uberoi 1957) or present in one direction only (e.g. Harris, Graham & Corrsin 1977 – hereinafter referred to as HGC); because of the relative simplicity of these flows, the inferences drawn from these estimates are not expected to be general. The present flow, while being sufficiently simple because of the normal and spanwise homogeneity (thus rendering the triple-correlation terms effectively zero), is sufficiently complex because of the two mean rates of strain (the shear as well as the acceleration) that some general conclusions could be expected from the pressure–strain terms deduced from energy balance. In particular, this would allow a direct assessment to be made of the adequacy or validity of some of the current models for these terms, especially those involving the linear or the mean strain part (or the 'rapid part', as it is often called). Leslie (1980), for example, has made a somewhat similar attempt for the HGC data.

Mention should here be made of the studies by Gence & Mathieu (1979) and Townsend (1980) both of which complement the present work. Gence & Mathieu (1979) studied the effect of successive irrotational distortion in a duct in which the principal axes of mean strain changed continuously. Townsend (1980) provided a scheme for calculating the response of sheared turbulence to additional distortion (for a brief description, see §4.3 below).

Briefly, then, the study consisted of the following. A homogeneous shear flow was generated using essentially the HGC setup and allowed to reach its asymptotic state. A two-dimensional contraction was inserted a short distance downstream. Both mean velocity and turbulence-stress profiles (normal and shear) were measured at several stations along the flow direction; some components of energy dissipation were also measured. The pressure–strain terms were evaluated from the energy balance made along the wind-tunnel axis. Although, with this information, it is in principle possible to test most existing pressure–strain models, we restricted ourselves to testing the following three: (*a*) Rotta's (1951, 1962) linear intercomponent exchange hypothesis; (*b*) the Daly & Harlow (1970) method of indirectly accommodating mean

strain rates; and (*c*) Launder *et al.*'s (1975) method of modelling the mean-strain part explicitly. Each of these models is representative in the sense that each adopts a different philosophy.

Two contractions, of effective area ratio 1.4 and 2.6, were used. The original intention had been to use three area ratios for the contraction so that the ratio of the longitudinal rate of strain to the mean shear in the flow was far less than, approximately equal to, and far greater than, unity. Unfortunately, the size of the wind-tunnel test section precluded consideration of this last case. However, this omission does not appear serious because the extra strain can then be expected to overwhelm the shear (see §4.3). Here the strain rate ratio was about 0.12 in the lower-area-ratio contraction (case *a*), and about 1 in the higher-area-ratio contraction (case *b*). In both cases, the strain fields – longitudinal as well as shear – were not large enough for the turbulence field to be treated by the rapid-distortion approach (e.g. Ribner & Tucker 1953; Batchelor & Proudman 1954; Townsend 1954; Hunt 1973, 1977) which requires that the external strain be applied so rapidly that the self-modulation and viscous terms have little time to become effective. However, it has often been found that, even when the externally applied strain rate is not strictly large, the rapid-distortion theories qualitatively reproduce the measured results (e.g. Townsend 1954, 1976; Narasimha & Sreenivasan 1973; Keffer *et al.* 1978) especially if the theory is 'corrected' for the 'natural development' of the flow. This idea has been used quite successfully in the past (e.g. Prabhu, Narasimha & Sreenivasan 1974; Tucker & Reynolds 1968; Townsend 1980). Encouraged by such attempts, we considered it worthwhile making a 'prediction' for the stress and energy components using the rapid-distortion approach and its modifications.

Section 2 provides details of the experimental facilities and measuring equipment. In §3, the measurements are presented; simple predictions for the mean velocity and turbulence stresses are attempted in §4. In §5, the pressure–strain terms are evaluated from approximate energy-balance measurements, and examined in the light of the models mentioned earlier. The note ends with a summary of some of the conclusions. In the appendix, we examine to what extent the concept of total strain can unify the homogeneous shear-flow measurements; this is in essence an update of the notion due to Townsend (1976).

2. Experimental conditions

The wind-tunnel and the shear generator used for the present experiments have been described by HGC. Briefly, the wind-tunnel has a 3.36 m long test section with a 30.5×30.5 cm nominal cross-section. The shear generator consists of twelve channels of equal width, whose variable resistance to the flow can be adjusted to create a linear mean velocity distribution some distance downstream. A two-dimensional contraction was created by placing two wedges symmetrically in the test section (see figure 1) beginning at $x_1/h \approx 7.6$, where $h(= 30.5$ cm) is the height of the test section. The wedges were made of polished wood except for the aluminium leading edges bonded to the main body. The mean centreline velocity upstream of the contraction ($x_1/h = 6.5$) was about 10.86 m s^{-1} in case (*a*) and 10.31 m s^{-1} in case (*b*), respectively about 12 % and 17 % below the HGC value. These reductions were caused by the insertion of the contraction wedges into the test section, and could not be eliminated because of the blower limitations. The mean shear rates in the flow at $x_1/h = 6.5$ were respectively 39 s^{-1} and 36 s^{-1}, also lower than the HGC value of 44 s^{-1}

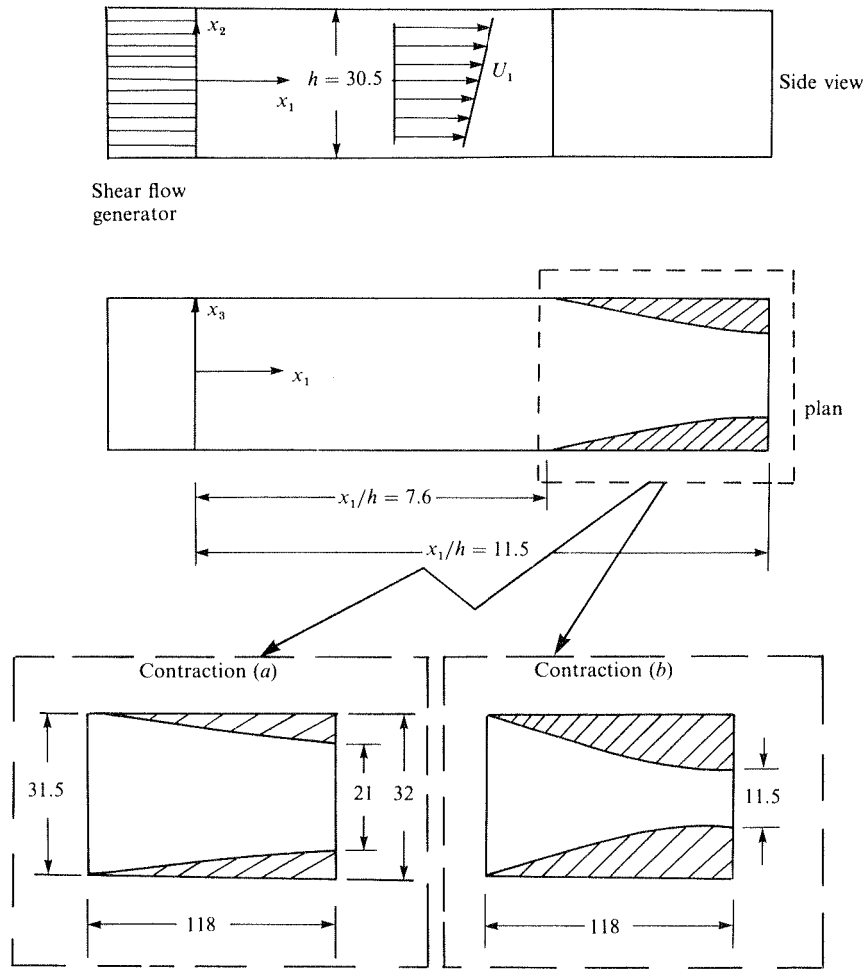

FIGURE 1. Schematic of the wind-tunnel and two-dimensional contractions. All dimensions in cm.

by about the same fractions as the mean velocity. The turbulence levels were also slightly lower, and these are described in §3.

The mean and turbulent velocities were measured with DISA 55D01 anemometers using Pt–Rh DISA X-wires, each 5 μm in diameter and about 0.8 mm in length. The X-wires were calibrated in the wind-tunnel without the shear generator in place, and the spanwise cooling of the hot wires was taken into account by using Champagne, Sleicher & Wehrmann's (1967) expression for the effective velocity U_e as

$$U_e = U_1 [\cos^2\phi + K^2 \sin^2\phi]^{\frac{1}{2}},$$

where ϕ is the angle of the wire to the flow direction, and K is assumed to be 0.2. The turbulence velocity signals were digitized on an 8-bit digitizer and processed on-line on a PDP 11/40 computer. In the earlier stages of the work, the signals were linearized on the digital computer, but it was discovered that the differences in the second moments between the linearized and nonlinear signals were small, and so the results presented here uniformly ignore linearization.

3. Measurements

3.1. *The asymptotic state of the linear shear flow*

For purposes of locating the wedges forming the contraction in the wind-tunnel, it is necessary to establish the streamwise distance beyond which the homogeneous shear flow can reasonably be said to have reached its asymptotic state. Although HGC observed that this state (identified essentially by the linear growths of $\overline{u_1^2}$, $\overline{u_2^2}$ and $\overline{u_3^2}$) is reached when the parameter $(x_1/\mathscr{U}_c)\,dU_1/dx_2$, $\mathscr{U}_c$ ($\equiv U_1$ at $x_2 = 0$) being the centreline velocity in the test section, exceeds a certain value, it is not exactly clear from their plots when this occurs. For the purpose of plotting the data in a more helpful way we note that, by definition, the ratios of different turbulent quantities to each other are constant with x_1 in the asymptotic state of the flow. The most appropriate quantities to examine then are the 'K parameters' (originally designated as structure parameters by Townsend 1954) defined as follows:

$$K_0 \equiv \frac{-\overline{u_1 u_2}}{\overline{u_k u_k}} \quad (k \text{ summed over } 1,2,3); \quad K_1 \equiv \frac{\overline{u_1^2}-\overline{u_2^2}}{\overline{u_1^2}+\overline{u_2^2}}; \quad K_2 \equiv \frac{\overline{u_1^2}-\overline{u_3^2}}{\overline{u_1^2}+\overline{u_3^2}}. \tag{2}$$

From figure 2, one can see that the asymptotic state is approximately reached for $(x_1/\mathscr{U}_c)\,dU_1/dx_2 \gtrsim 5$. For the present experiments, this means that $x_1/h \gtrsim 6$. HGC estimated from their plots that the asymptotic state was attained around $(x_1/\mathscr{U}_c)\,dU_1/dx_2 \approx 7$, a similar but slightly more conservative conclusion.

To allow the flow to develop further, and to account for possible upstream influence due to the contraction, it would be preferable to have the contraction begin at a somewhat larger x_1/h. In these experiments, the wedges were placed at $x_1/h \simeq 7.6$, and the contraction effects were just noticeable from $x_1/h \simeq 7$. The range of the present measurements is thus $7 \lesssim x_1/h \lesssim 11$.

3.2. *Mean velocity distributions*

Figure 3 shows the mean velocity profiles across the test section measured at several locations along the contraction. About a 5 cm region in the vicinity of the top and bottom walls was excluded from measurements so as to avoid possible confusion with the boundary influence. The mean-velocity distribution maintains its linear shape throughout, and becomes progressively less steep as the flow develops through the contraction.

3.3. *Turbulence stresses*

Figure 4 shows the variation of the root-mean-square velocity fluctuations u_1', u_2' and u_3', normalized by the local centreline velocity $\mathscr{U}_c$. Figure 5 is a plot of the normalized Reynolds shear stress $-\overline{u_1 u_2}/\mathscr{U}_c^2$; in this plot, the inhomogeneities present in the flow are exaggerated in comparison with those of normal stresses. (The correlation coefficient C defined by (1), however, remains more uniform in x_2 than the turbulent intensities or the shear stress individually.) The degree of normal homogeneity generally improves with streamwise distance. *Roughly* speaking, we can conclude from figures 3, 4 and 5 that a uniformly sheared flow that initially has an approximate homogeneity retains this property throughout the contraction.

Referring to figure 1, the relatively small width of the test section towards the end of contraction (*b*) makes it necessary to ascertain that there indeed was a central region within which homogeneity in the x_3-direction is a reasonable approximation. Figure 6 shows two profiles of $u_1'/\mathscr{U}_c$ at $x_1/h = 9.5$ and 11; also marked are the 'edges' of the side-wall boundary layers, as determined from mean-velocity measurements.

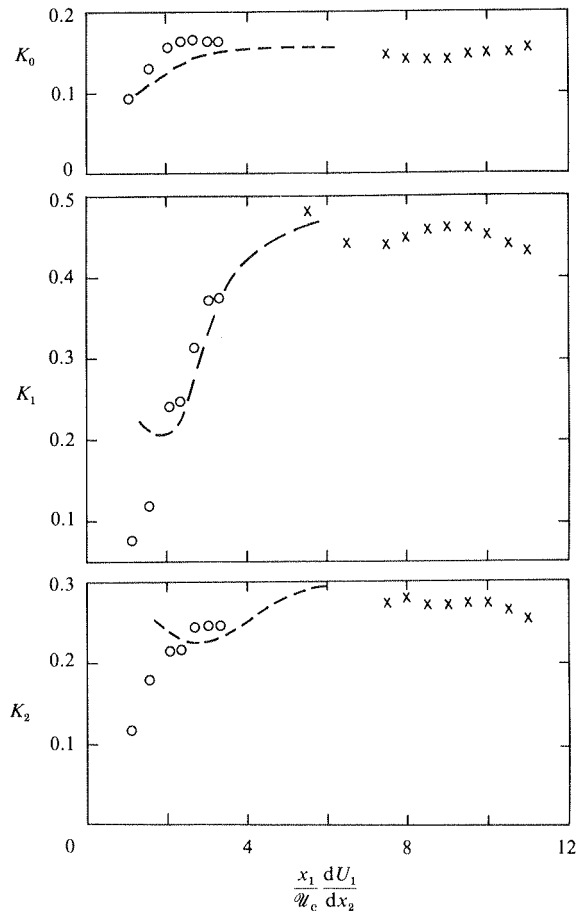

FIGURE 2. Variation of the structural parameters K_0, K_1 and K_2 against $(x_1/\mathscr{U}_c)(dU_2/dx_2)$: ○, Champagne *et al.* (1970); ×, Harris *et al.* (1977); ---, Mulhearn & Luxton (1975).

At the last measuring station, there is a central 5 cm region where variations in the mean velocity U_1 are negligible. However, the extent of this region for turbulent intensities is less (because of the boundary-layer-induced 'potential' fluctuations), and is no more than about 2 cm long. The assumption of homogeneity in the x_3-direction is therefore less certain towards the end of contraction (b),† although no more so than that of homogeneity in the x_2-direction. It is, however, necessary to comment that attempts were made using Phillips' (1955) $\frac{1}{4}$-power law to correct for the 'potential' fluctuations due to the side-wall boundary layers, but the corrections did not have a significant influence on any of the conclusions that follow.

† A possible implication is that the largest scales of motion may be inhomogeneous, although this should not seriously affect the energy-containing range of eddies.

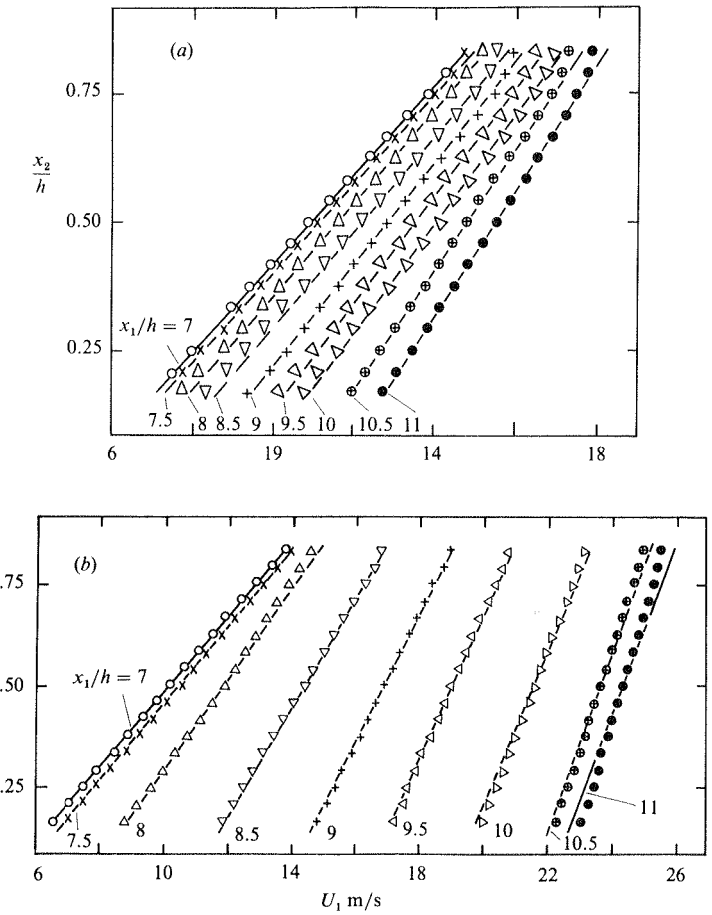

FIGURE 3. Mean velocity profiles across the wind-tunnel through the contractions (a) and (b). Straight lines correspond to predictions from the application of Bernoulli's equation along fixed streamline (see §4.1).

4. Prediction and analysis of measurements

4.1. *Mean-velocity distribution*

The mean-velocity development in the contraction can be predicted relatively easily by the use of Bernoulli's equation, which should hold reasonably well along streamlines in an environment of low turbulence level such as the present flows. First, because the mean velocity is everywhere linearly distributed, we can write

$$U_1 = \mathscr{U}_c + \frac{\partial U_2}{\partial x_2} x_2, \tag{3}$$

where the suffix c denotes centreline values. Upon integrating (3) across the wind-tunnel height, conservation of mass requires (ignoring the boundary-layer development) that

$$\mathscr{U}_c \approx A\mathscr{U}_{co}. \tag{4}$$

Here, the additional suffix o refers to a station upstream of the contraction and A

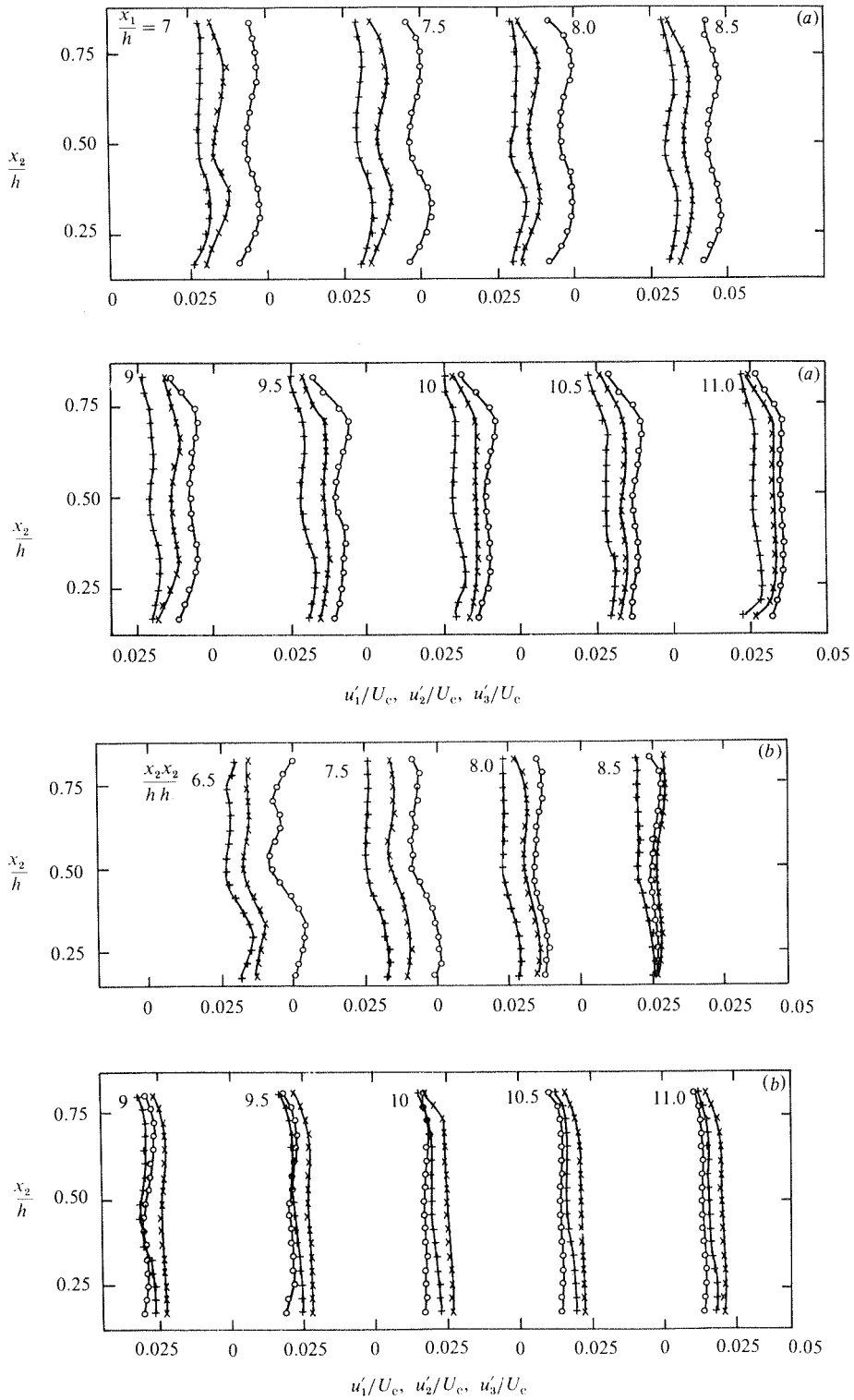

FIGURE 4. Normalized turbulent root-mean-square intensity profiles for contractions (*a*) and (*b*): ○, u_1'/U_c; +, u_2'/U_c; ×, u_3'/U_c.

FIGURE 5. The normalized Reynolds shear stress distribution $-\overline{u_1 u_2}/\mathscr{U}_c^2$ through contractions (*a*) and (*b*). For clarity, points are joined by lines and the origin on the abscissa is shifted for each set of points.

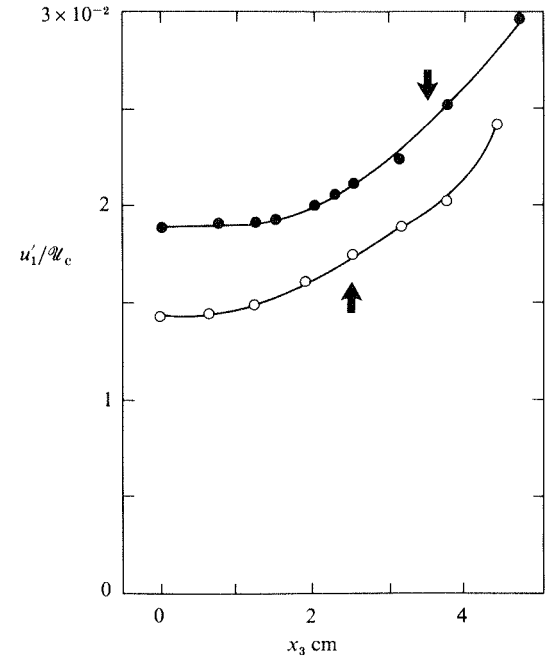

FIGURE 6. Spanwise distribution of turbulent intensity $u_1'/\mathscr{U}_c$ for contraction (*b*). ●, $x_1/h = 9.5$; ○, 11. The arrows show the 'edge' of the sidewall boundary layer (as measured by mean velocity distribution).

is the (effective) local area ratio (>1). Applying Bernoulli's equation along a mean streamline (which in this case resides at a constant x_2/h), we have

$$U_1^2 = \frac{2}{\rho}(P_0 - P) + U_{10}^2, \tag{5}$$

where P is the static pressure and ρ is the density. Since $P_0 - P$ is independent of x_2, it follows from (5) that

$$\frac{\partial U_1}{\partial x_2} = \frac{U_{10}}{U_1}\left(\frac{\partial U_1}{\partial x_2}\right)_0 = \frac{1}{A}\left(\frac{\mathrm{d}U_1}{\mathrm{d}x_2}\right)_0. \tag{6}$$

It now follows from (3), (6) and (4) that

$$U_1 = A\mathscr{U}_{\mathrm{co}} + \frac{x_2}{A}\left(\frac{\mathrm{d}U_1}{\mathrm{d}x_2}\right)_0, \tag{7}$$

all quantities on the right-hand side of (7) being known. Figure 3 shows that the mean-velocity profiles obtained from (7) are in good agreement with measurement except perhaps towards the end of the contraction (b). This is not surprising since the stream surfaces diverge some distance upstream of the geometric end of the contraction, so that the approximation that they reside along surfaces of constant x_2/h becomes less accurate.

4.2. *Energy and stress balance*

Homogeneity in the normal and spanwise directions implies little turbulence transport, and the viscous transport is negligible if the Reynolds number is high. HGC have written the turbulence-component energy equations to the leading order as relevant to a transversely homogeneous shear flow. Transverse homogeneity is a reasonable approximation in the flows considered here (in fact, better than in the HGC flow), and many of the consequences they deduce hold at least as well. It is perhaps necessary to comment a little on the spanwise homogeneity which requires, typically, that:

$$\frac{\partial}{\partial x_3}\overline{(q^2 u_3)} = \frac{\partial}{\partial x_3}\overline{(u_3 p)} = 0,$$

where $\overline{q^2} = \overline{u_k u_k}$ and p is the fluctuating pressure. These relations may not be strictly true towards the late stages of contraction (b), but elsewhere in case (b), as well as in case (a), they must be reasonably good because there is a sufficiently wide region in the x_3-direction within which turbulence properties are essentially constant.

A second comment concerns turbulent transport in the streamwise direction. Measurements have shown, in both contractions (a) and (b), that

$$\left|\frac{(\partial/\partial x_1)\,\overline{(u_1 q^2)}}{\mathscr{U}_c\,\partial\overline{u_1^2}/\partial x}\right| \lesssim 0.05,$$

so that it is possible to ignore to a very good approximation terms like $(\partial/\partial x_1)\,\overline{(u_1 q^2)}$. Similarly, it appears reasonable to put

$$\frac{\partial}{\partial x_1}\overline{(u_1 p)} \approx 0.$$

This term is at most of the order $p'q'/l$, where $q' = [\overline{(q^2)}]^{\frac{1}{2}}$ and l is an integral scale of turbulence; l/q' is a characteristic eddy turnover timescale. The ratio $p'q'/l$ is clearly smaller than the term $\overline{p(\partial u_1/\partial x_1)}$, which would be at least of the order $p'q'/\lambda$

(λ is the Taylor microscale). Further, the viscous diffusion term $\nu(\partial/\partial x_1^2)\,(\overline{q^2})$ was actually computed from the $\overline{q^2}$ data, and was found to be small. Following the lead of HGC, the relevant equations can then be written as:

$$U_1\frac{\partial(\frac{1}{2}\overline{u_1^2})}{\partial x_1} \approx -\overline{u_1 u_2}\frac{\partial U_1}{\partial x_2} - \overline{u_1^2}\frac{\partial U_1}{\partial x_1} + \overline{\frac{p}{\rho}\frac{\partial u_1}{\partial x_1}} - \epsilon_1; \tag{8}$$

$$U_1\frac{\partial(\frac{1}{2}\overline{u_2^2})}{\partial x_1} \approx \overline{\frac{p}{\rho}\frac{\partial u_2}{\partial x_2}} - \epsilon_2, \tag{9}$$

and

$$U_1\frac{\partial(\frac{1}{2}\overline{u_3^2})}{\partial x_1} \approx \overline{u_3^2}\frac{\partial U_1}{\partial x_1} + \overline{\frac{p}{\rho}\frac{\partial u_3}{\partial x_3}} - \epsilon_3, \tag{10}$$

where

$$\epsilon_\alpha = \nu\,\overline{\frac{\partial u_\alpha}{\partial x_k}\left(\frac{\partial u_\alpha}{\partial x_k} + \frac{\partial u_k}{\partial x_\alpha}\right)}, \quad \alpha = 1, 2 \text{ or } 3 \tag{11}$$

(here and elsewhere no summation is implied on α) indicate the viscous dissipation terms. Compared with the HGC flow, we can expect a slower streamwise growth of $\overline{u_1^2}$ because of the reduced $\partial U_1/\partial x_2$ (see (5)), and the appearance of the extra (negative) term $-\overline{u_1^2}\,\partial U_1/\partial x_1$ on the right-hand side. On the other hand, $\overline{u_3^2}$ can be expected to grow faster than in the HGC case because of the $\overline{u_3^2}\,\partial U_1/\partial x_1$ term in (10). These expectations are generally consistent with observations.

To the same degree of approximation, the balance equation for the Reynolds shear stress can be written as

$$U_1\frac{\partial(-\overline{u_1 u_2})}{\partial x_1} \approx \overline{u_1 u_2}\frac{\partial U_1}{\partial x_1} + \overline{u_2^2}\frac{\partial U_1}{\partial x_2} - \overline{\frac{p}{\rho}\left(\frac{\partial u_1}{\partial x_2} + \frac{\partial u_2}{\partial x_1}\right)}. \tag{12}$$

If the Reynolds number is sufficiently large, the viscous terms in this equation can be expected to be negligible (Champagne *et al.* 1970). The only extra term here from the corresponding HGC equation is the $\overline{u_1 u_2}(\partial U_1/\partial x_1)$ term. The negative magnitude of this term suggests that $-\overline{u_1 u_2}$ increases more slowly than in the unaccelerated shear flow, again as observed.

The turbulent kinetic-energy equation is

$$U_1\frac{\partial(\frac{1}{2}\overline{q^2})}{\partial x_1} \approx -\overline{u_1 u_2}\frac{\partial U_1}{\partial x_2} - (\overline{u_1^2} - \overline{u_3^2})\frac{\partial U_1}{\partial x_1} - \epsilon, \tag{13}$$

where the viscous dissipation term $\epsilon = \epsilon_1 + \epsilon_2 + \epsilon_3$.

4.3. *Rapid-distortion calculations*

An important factor to be noted in (8)–(10), (12) and (13) is that the self-modulation effects of turbulence occur only through pressure in the pressure–strain covariance terms, but that is enough to render the first-principle prediction of the turbulence stresses impossible. If the mean strain rates are sufficiently rapid, this effect becomes negligible, and the evolution of turbulent-energy components can be predicted completely from linear theory alone. For this rapid-distortion assumption to hold for the energy-containing eddies, it is necessary that the superimposed strain have a characteristic timescale much smaller than that characteristic of the energy containing eddies. This latter quantity can be expected to be of the order (l/q'), and thus the appropriate ratios to examine are (i) $(q'/l)/(\partial U_2/\partial x_2)$ for the mean shear, and (ii) $(q'/l)/(\partial U_1/\partial x_1)$ for the longitudinal strain. With increasing distance into the contraction, the mean shear $\partial U_1/\partial x_2$ becomes smaller, while the longitudinal strain rate $\partial U_1/\partial x_1$ increases initially before settling down to be a constant. (Towards the very

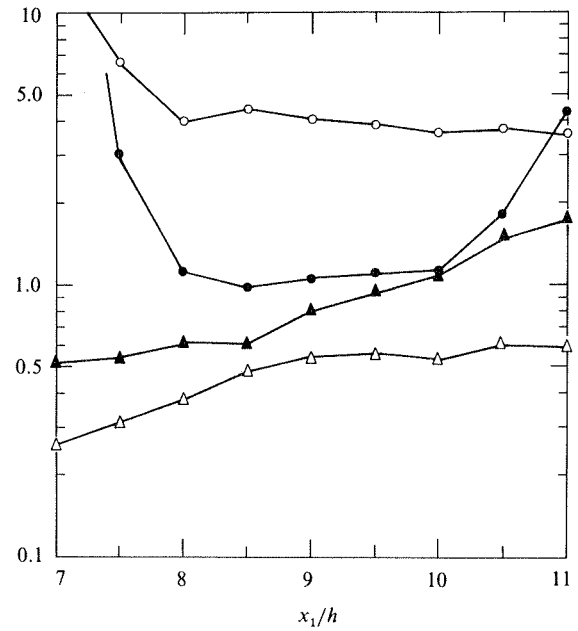

FIGURE 7. The parameters $(q'/l)/(\partial U_1/\partial x_1)$ (○, ●), and $(q'/l)/(\partial U_1/\partial x_2)$ (△, ▲) during contraction. Unfilled and filled symbols correspond respectively to contractions (*a*) and (*b*).

end of the contraction (*b*), $\partial U_1/\partial x_1$ also falls off.) Figure 7 shows the ratios (i) and (ii) defined above; here, l is determined from $\frac{1}{3}(q')^3/\epsilon$. It is seen that, for the contraction (*a*), the mean shear is an order of magnitude larger than the mean streamwise acceleration, while both of them are comparable in case (*b*). None of the straining rates in either contraction is sufficiently large for rapid-distortion theory to be strictly applicable, but it is known (e.g. Townsend 1954, 1976; Narasimha & Sreenivasan 1973; Keffer *et al.* 1978) that, even if the rapid distortion requirements are only marginally satisfied, the evolution of the turbulence structure is qualitatively consistent with the rapid-distortion hypothesis. Explicit results are available only for simple types of distortion, such as irrotational distortion (see Batchelor & Proudman (1954) for initially isotropic turbulence, Sreenivasan & Narasimha (1978) for initially axisymmetric turbulence) and plane shearing (Pearson 1959; Townsend 1976), but not for complex distortions such as occur in the present experiments. The one exception is due to Townsend (1980), who evolved a step-by-step procedure to account for a combination of several simple distortions; according to this procedure, the distortion history is split into a number of steps, each of a simple type and not too large, chosen so that the total distortion at the end of each step is reasonably close to the actual flow distortion. Powerful though this procedure is, actual calculations assume an arbitrarily chosen eddy viscosity (Pearson 1959; Townsend 1976) to account for the energy transfer from large to small eddies.

An appropriate scheme for calculating the present flow is one in which the condition just upstream of contraction are assumed to have evolved from an hypothetical isotropic state under the application of plane shear (Townsend 1976) and then apply the step-by-step procedure of Townsend (1980). We have not done this for two reasons. First, our objective here is relatively simple and restricted in scope: we want to demonstrate that, although the shear is at least as strong as irrotational strain,

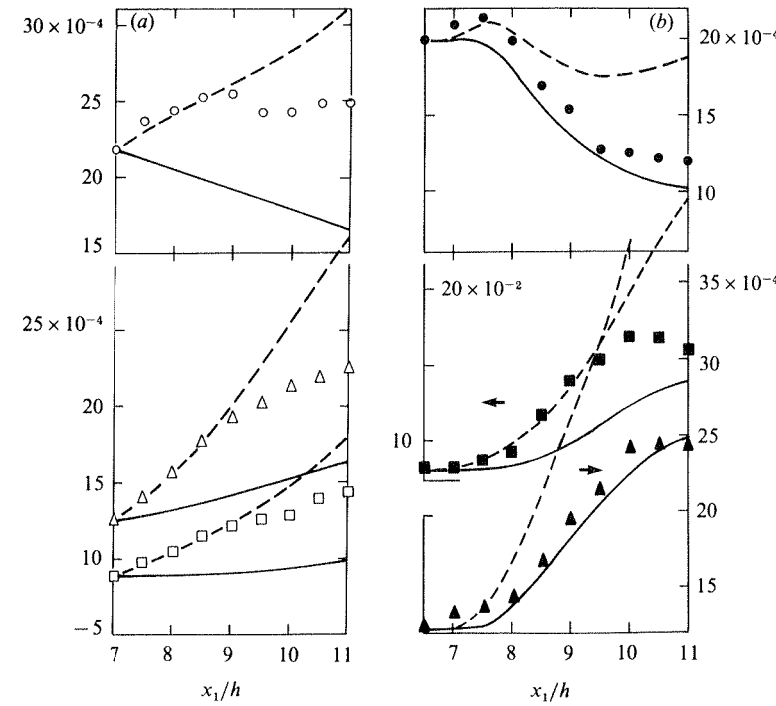

FIGURE 8. Variation of turbulent intensities along the wind-tunnel axis through the contraction. Open symbols for contraction (*a*), and closed symbols for contraction (*b*). Note staggered origins. ○, $\overline{u_1^2}/\mathscr{U}_{co}^2$; □, $\overline{u_2^2}/\mathscr{U}_{co}^2$; △, $\overline{u_3^2}/\mathscr{U}_{co}^2$. ——, from irrotational rapid-distortion theory; – – –, with modifications for natural development.

the latter quantity has a dominating influence on the evolution of turbulence structure for a certain distance following its application. Secondly, the scheme described above assumes (for tractability) that the plane shear is rapid, which it is not in the present experiments. The resulting uncertainty of these calculations will thus introduce an ambiguity in the interpretation of the present analysis whose chief concern is a qualitative assessment of which of the two strains within the contraction has a dominating influence. Under the circumstances, it seemed instructive to calculate the effects of the irrotational and shear strains separately, instead of resorting to complex schemes which combine both.

The rapid distortion results for the irrotational strain are shown in figure 8. Here, for simplicity, we have used 'isotropic theory', and scaled the individual components to the appropriate measured values at $x/h = 7$, thus necessarily forcing at the starting point perfect agreement between experiment and theory. Allowing for this artifact, we may note that the theory seems to be quite successful for $\overline{u_1^2}$ and $\overline{u_3^2}$ in case (*b*), although it uniformly underestimates $\overline{u_2^2}$. Not unexpectedly, even the qualitative behaviour is not predicted correctly for the contraction (*a*).

Since the irrotational strain in the present experiments if far from being rapid in the strict sense – see e.g. Hunt (1973) for a thorough discussion of the conditions for rapidity – it is interesting to see whether the conclusions change if one allows for the 'natural development' of the flow in some empirical way. Although the 'correction' procedure we adopt is much the same in spirit as that of Ribner & Tucker (1953), we note that we are not merely correcting for viscous decay, but for the development that would have occurred in the absence of the contraction.

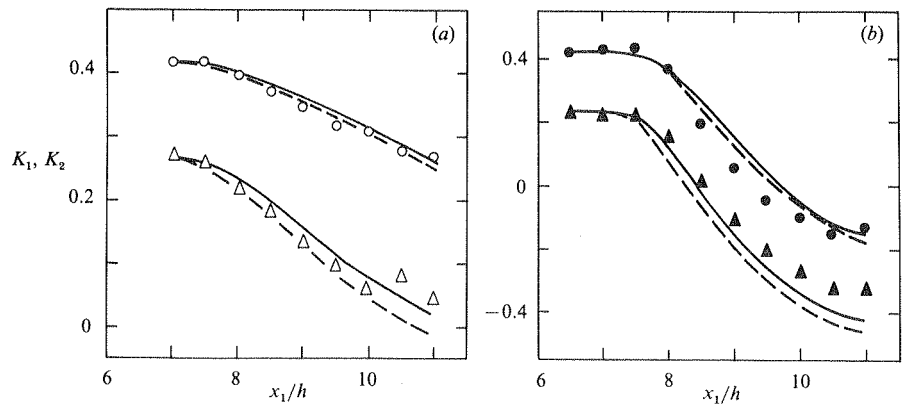

FIGURE 9. Variation of the structural parameters K_1 (○, ●) and K_2 (△, ▲) through the contraction. Curves as in figure 8.

Let f_α indicate the ratio $\overline{u_\alpha^2}/(\overline{u_\alpha^2})_0$ ($\alpha = 1, 2$ or 3, not summed) corresponding to the situation when the homogeneous shear flow develops undistorted, such as in the HGC experiment. Further, let g_α indicate the same ratio predicted according to the rapid-distortion theory discussed above. The product $f_\alpha g_\alpha$ then gives the combined effect of the natural development of the flow and of rapid distortion, assuming that the two effects occur separately. Figure 8 also shows that these 'modified rapid-distortion' results are acceptable for $x_1/h \lesssim 9$ in case (a); although the general agreement for $\overline{u_2^2}$ in case (b) improves, the prediction for the other two components is worse. The reason is clearly that the 'corrections' are too large, or that the two effects – the rapid distortion and the natural development – do not occur independent of each other.

The usefulness of the rapid-distortion theory is not that it can provide a working-prediction model for energy-component changes in situations such as the present one, but that it can predict the K parameters correctly. Figure 9 shows that both sets of calculations give reasonable results for K_1 and K_2, which are thus insensitive to the specific model.

Let us now consider the shear strain separately. As mentioned earlier, we can view the turbulence structure just upstream of contraction as evolving from a (hypothetical) initially isotropic state in response to the application of mean shear. Similarly, the turbulence structure anywhere within the contraction can also be viewed as developing from a structureless state through the application of the appropriate strain history. If the applied mean shear strain is sufficiently large, the turbulence structure at any given stage is completely determined by the local value of the total strain parameter

$$\beta = \int_0^{T'} (\partial U_1/\partial x_2)\, \mathrm{d}t;$$

T', typically the lifetime of the large eddy, is the order of $\frac{1}{3}\overline{q^2}/\epsilon$ in equilibrium, so that $\beta \approx \frac{1}{3}(\overline{q^2}/\epsilon)\,(\partial U_1/\partial x_2) \approx 4.5$ just upstream of contraction. During contraction, $(\partial U_1/\partial x_2)$ decreases with x_1 (see figure 3), but large eddies will still have a timescale not very different from the initial value; the net result is that, towards the end of contraction, $\beta \approx 1.5$ for contraction (a) and about 2.5 for contraction (b). According to the rapid-distortion hypothesis, the turbulence energy components as well as the

Reynolds shear stress upstream of the contraction should correspond to a $\beta \simeq 4.5$, while those downstream must correspond to the respective downstream values of β estimated above; anywhere inside the contraction, one can use the local values of $\partial U_1/\partial x_2$ to evaluate the local β which should be sufficient to specify the turbulence structure there.† As remarked elsewhere, Townsend (1976, chapter 3; for example, figure 3.14) has calculated the variation of energy components with β. We shall, however, avoid making a detailed comparison of these calculations and the measurements, chiefly because of the uncertainty in the precise value of β (one can only make estimates for it) and the sensitivity of the quantitative results to it. Brief calculations suggest that: for contraction (a) the energy components $\overline{u_1^2}$ and $\overline{u_3^2}$ should decrease respectively at the end of contraction to about $\frac{1}{4}$ and $\frac{1}{2}$ of their pre-contraction values, while $\overline{u_2^2}$ should increase by a factor of about 1.7; for contraction (b) $\overline{u_1^2}$ and $\overline{u_3^2}$ should decrease respectively to about $\frac{1}{2}$ and $\frac{2}{3}$ of their initial values and $\overline{u_2^2}$ should increase by a factor of about 1.5. Except for $\overline{u_2^2}$ and $\overline{u_1^2}$ in case (b), even the direction of these predictions is wrong (see figure 9).

Corrections of the type mentioned above bring the results into qualitatively better agreement with measurement, but the overall performance still falls short of the corresponding irrotational rapid-distortion calculations (except perhaps for $\overline{u_1^2}$ in case (b)). The relatively better performance of the irrotational rapid-distortion theory as compared to the shear rapid-distortion theory, even though the shear strain is at least as rapid as the longitudinal strain, should be attributed essentially to the well-known fact that the turbulence structure responds more readily to the extra strain even when its absolute value is smaller.

Figure 10 shows the variation of the Reynolds shear stress $-\overline{u_1 u_2}$ along the centreline (the lower two blocks) as well as the correlation coefficient C (the uppermost block) which seems to remain nearly constant – only a little higher than the corresponding HGC value in the undistorted homogeneous shear flow. The irrotational rapid-distortion theory is incapable of evaluating the shear-stress variations, but the fact that the measured correlation coefficient is approximately constant through the contractions implies that the Reynolds stress variation is given simply by changes in the velocity product $u_1' u_2'$. By this hypothesis, the irrotational rapid-distortion results give

$$-\overline{u_1 u_2} = C_0 (g_1 g_2)^{\frac{1}{2}} \tag{14}$$

while the modified results give

$$-\overline{u_1 u_2} = C_0 (f_1 f_2)^{\frac{1}{2}} (g_1 g_2)^{\frac{1}{2}}. \tag{15}$$

Here, C_0 is the pre-contraction value of the correlation coefficient C. These calculations are also shown in figure 10, using the measured value of C_0 (0.49 in case (a) and 0.45 in case (b)). There is reasonable agreement for $x_1/h \lesssim 9$ in both contractions (a) and (b). The shear rapid-distortion calculations, on the other hand, suggest that $-\overline{u_1 u_2}$ should actually decrease (to about $\frac{1}{2}$ and $\frac{2}{3}$ the initial values, respectively, in cases (a) and (b)) if no correction is applied, and that it shall remain approximately constant if the previously discussed corrections are applied. Both these predictions are incorrect, again presumably because of the reasons mentioned earlier.

† This view is strictly correct only for a flow in equilibrium (see § A 3). See Maxey (1982) for ways of handling 'non-equilibrium' situations. For present purposes, such modifications were deemed unnecessary.

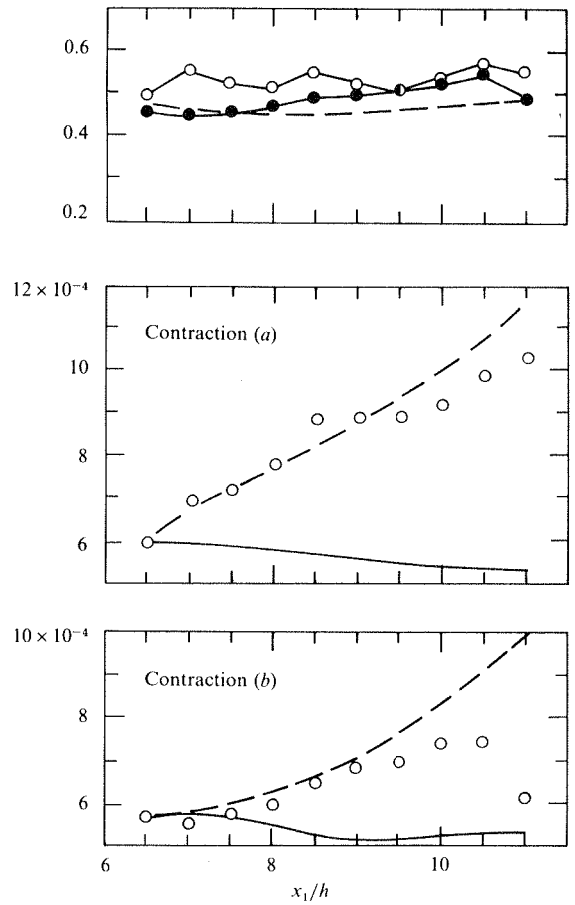

FIGURE 10. Variation of the correlation coefficient C and the normalized Reynolds shear stress $-\overline{u_1 u_2}/\mathscr{U}_{c0}^2$ (○, contraction (a); ●, contraction (b)) along the wind-tunnel axis through the contraction. In the top figure, data points are joined only for clarity; ---, mean HGC data. In the lower two figures, curves indicate calculations according to (14) (——) and (15) (– – –).

5. Pressure–rate-of-strain covariances

To evaluate by balance the pressure–strain terms from (8)–(10) and (12), it is necessary to measure all other terms in these equations. We measured some (but not all) components of the fractional energy dissipation rates ϵ_α (see (11)), and all other quantities of interest. The total energy dissipation rate $\epsilon = \epsilon_1 + \epsilon_2 + \epsilon_3$ can however be obtained fairly easily from (13) in which every other quantity has been measured. The ϵ thus estimated along the centreline is compared in figure 11 with the isotropic estimate

$$\epsilon_{\mathrm{I}} = 15\nu \overline{\left(\frac{\partial u_1}{\partial x_1}\right)^2}, \tag{16}$$

where $\partial u_1/\partial x_1$ is obtained from the temporal derivative of u_1 using the Taylor approximation

$$\frac{\partial}{\partial x_1} = \frac{1}{\mathscr{U}_c}\frac{\partial}{\partial t}.$$

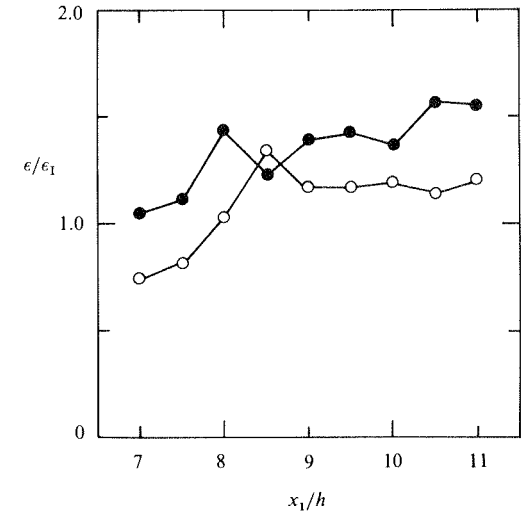

FIGURE 11. The ratio of the turbulent energy dissipation ϵ obtained by energy balance to that obtained by local isotropy. ○, contraction (a); ●, contraction (b).

Figure 11 shows that one of the effects of the contraction is to enhance the rate of dissipation beyond the isotropic value ϵ_{I}. Somewhat larger deviations from local isotropy in case (b) indicate a possibility that the additional strain due to acceleration affects the dissipating range of eddies directly; this is not unexpected at the moderate Reynolds numbers ($R_\lambda \equiv u_1'\lambda/\nu \simeq 250$ at $x_1/h = 6.5$) of the flow. A further indication that the assumption of isotropic dissipation is not strictly applicable comes from figure 12 which shows the ratios

$$\overline{\left(\frac{\partial u_2}{\partial x_1}\right)^2}\Big/\overline{\left(\frac{\partial u_1}{\partial x_1}\right)^2} \quad \text{and} \quad \overline{\left(\frac{\partial u_3}{\partial x_1}\right)^2}\Big/\overline{\left(\frac{\partial u_1}{\partial x_1}\right)^2}, \tag{17}$$

both of which should be 2 for local isotropy.

Although the isotropic estimates of dissipation thus are not strictly correct, the largest value of the ratio $\epsilon/\epsilon_{\mathrm{I}}$ is about 1.5, and neither of the quantities in (17) is more than about 20 % away from the isotropic value. Thus, if we put

$$\epsilon_1 \approx \epsilon_2 \approx \epsilon_3 \approx \tfrac{1}{3}\epsilon, \tag{18}$$

we may speculate that about 20 % errors in ϵ_α are likely.

After some trials with the measurement of all components of ϵ_α, we concluded that the errors could not be any less in these measurements (for a discussion of these errors in the context of temperature dissipation measurements, see Sreenivasan, Antonia & Danh 1977), and hence resorted to (18) for evaluating the pressure–strain terms from (8)–(10) and (12).

It is worth recalling that the pressure–strain terms at a position $\boldsymbol{x}$ can be expressed (Chou 1945) as:

$$\overline{\frac{p}{\rho}\frac{\partial u_i}{\partial x_j}} = \frac{1}{4\pi}\int_v \left\{\overline{\left(\frac{\partial^2 u_k u_l}{\partial x_k \partial x_l}\right)'\frac{\partial u_i}{\partial x_j}} + 2\left(\frac{\partial U_k}{\partial x_l}\right)\overline{\left(\frac{\partial u_m}{\partial x_k}\right)'\left(\frac{\partial u_i}{\partial x_j}\right)}\right\}\frac{\mathrm{d}\boldsymbol{x}'}{|\boldsymbol{x}-\boldsymbol{x}'|} + S_{ij}, \tag{19}$$

where the quantities with a prime are evaluated at $\boldsymbol{x}'$. The surface integral S_{ij} is vanishingly small except close to a solid boundary, and will be ignored here. The first

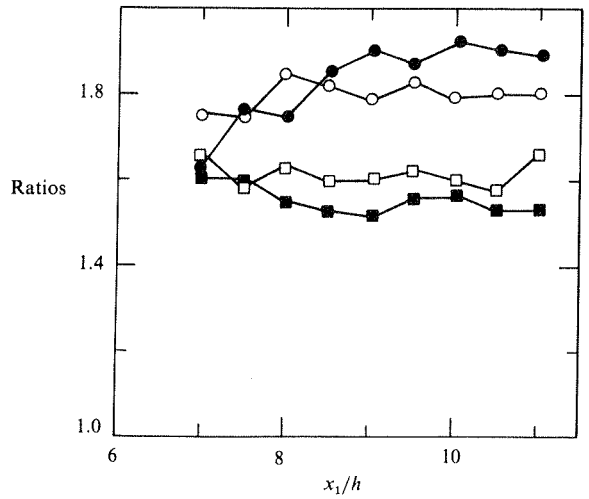

FIGURE 12. The squares represent the ratio $\overline{(\partial u_2/\partial x_1)^2}/\overline{(\partial u_1/\partial x_1)^2}$ and the circles the ratio $\overline{(\partial u_3/\partial x_1)^2}/\overline{(\partial u_1/\partial x_1)^2}$. Open symbols for contraction (a) and closed symbols for contraction (b).

term in (19) arises due to the self-interaction of turbulence while the second arises due to the interaction of turbulence with the mean shear.

Perhaps the most commonly used model for $\overline{(p/\rho)(\partial u_i/\partial x_j)}$ is that due to Rotta (1951, 1962) whose model for the first term in (19) (the only non-vanishing term in unstrained turbulence) is:

$$\overline{\frac{p}{\rho}\left(\frac{\partial u_i}{\partial x_j}+\frac{\partial u_j}{\partial x_i}\right)} = -c_1\left(\frac{\epsilon}{q^2}\right)(\overline{u_i u_j}-\tfrac{1}{3}\overline{q^2}\delta_{ij}). \tag{20}$$

If $c_1 > 0$, the diagonal terms imply a tendency towards energy equipartition. (The off-diagonal terms are also explicitly modelled by (20), although the physical mechanism is not clearly identifiable.) From an examination of Uberoi's (1957) data on homogeneous turbulence relaxing to isotropy downstream of axisymmetric contractions, Rotta (1962) obtained a value of about 2.8 for c_1. There were early speculations (e.g. Donaldson 1971) that the first term in (19) is the major contributor to the pressure–strain terms (with the constant c_1 perhaps taking a value different from 2.8), but this notion, however, is no longer seriously considered to be adequate (e.g. Reynolds 1976; Lumley & Khajeh-Nouri 1974). Lumley (1978) has argued that c_1 should indeed be a function of certain invariants formed from the strain tensor. At least one attempt has been made in the past (Daly & Harlow 1970) to incorporate implicitly the influence of mean rates of strain in c_1 by letting it be a function of the ratio of production rate $\mathscr{P}$ to the dissipation rate ϵ of the turbulent kinetic energy. This model implies, in its simplest form, that

$$c_1 = a(1+b\mathscr{P}/\epsilon), \tag{21}$$

where a and b are constants. If the production is zero, $a = c_1$ and Rotta's hypothesis is recovered.

One of the models incorporating the mean strain rates explicitly on a fairly general basis is due to Launder *et al.* (1975). This model appears to be finding its way into many computational schemes (see e.g. *Proceedings of the Stanford Conference on Complex Turbulent Flows, 1981*) and deserves careful consideration. According to the model, the second term of the volume integral in (19) is written as

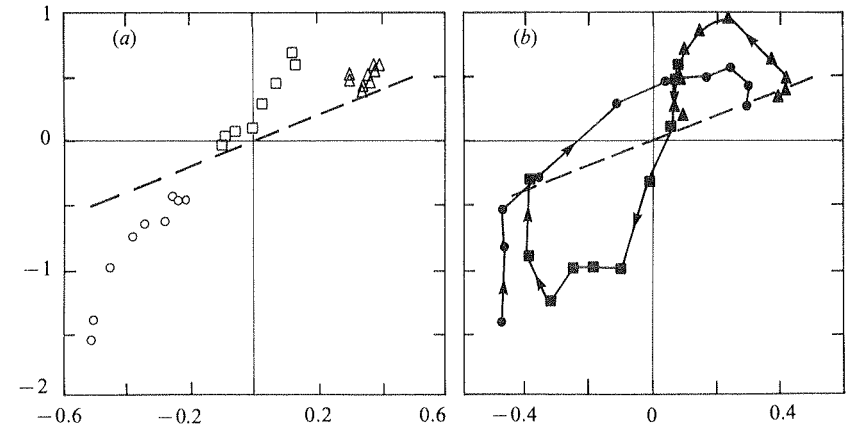

FIGURE 13. Test for Rotta's linear intercomponent energy-transfer hypothesis. Ordinate represents energy gain due to the pressure–strain terms, and the abscissa represents the energy loss according to Rotta's model. ---- according to Rotta's calculations from Uberoi's data. Open symbols for contraction (a) and filled symbols for contraction (b).

	Ordinate	Abscissa
Circles	$\epsilon^{-1}\overline{(p/\rho)(\partial u_2/\partial x_1)}$	$1-3\overline{u_1^2}/\overline{q^2}$
Triangles	$\epsilon^{-1}\overline{(p/\rho)(\partial u_2/\partial x_2)}$	$1-3\overline{u_2^2}/\overline{q^2}$
Rectangles	$\epsilon^{-1}\overline{(p/\rho)(\partial u_3/\partial x_3)}$	$1-3\overline{u_3^2}/\overline{q^2}$

Lines are drawn through data in (b) only to improve clarity.

$$-\gamma(\mathscr{P}_{ij}-\tfrac{2}{3}\mathscr{P}\delta_{ij}),\dagger \tag{22}$$

where γ is a constant, and

$$\mathscr{P}_{ij} = -\left\{\overline{u_i u_k}\frac{\partial U_j}{\partial x_k}+\overline{u_j u_k}\frac{\partial U_i}{\partial x_k}\right\}; \quad \mathscr{P} = \tfrac{1}{2}\mathscr{P}_{ii}.$$

Here, we restrict ourselves to the testing of (20), (21) and (22); other models (e.g. Lumley & Khajeh-Nouri 1974; Gibson & Launder 1978) do exist but are not considered here.

For the diagonal terms, we can write (20) as

$$\frac{1}{\epsilon}\overline{\frac{p}{\rho}\frac{\partial u_\alpha}{\partial x_\alpha}} = c\left(1-\frac{\overline{3u_\alpha^2}}{q^2}\right), \quad c = \tfrac{1}{3}c_1, \tag{23}$$

with no summation on α. Figure 13 shows $\epsilon^{-1}\overline{(p/\rho)(\partial u_\alpha/\partial x_\alpha)}$, $\alpha = 1, 2, 3$, evaluated from energy balance (with ϵ obtained from (13)) plotted against $(1-3\overline{u_\alpha^2}/\overline{q^2})$. Also shown are lines appropriate to Rotta's choice of c. Rotta implied that the constant c is the same for all three components in unstrained turbulence. If one *insists* on applying Rotta's hypothesis for the present flows with mean rates of strain, it is clear that no single value of c will be adequate for all three components. As has been pointed out for example by Leslie (1980), this insistence is an over-rigorous interpretation

† Near the wall the same model is more involved, but that is outside the scope of the present considerations.

of Rotta's model, and is included here only for the purposes of comparison with the previous analysis of HGC and Champagne *et al.* (1970). These authors have also determined that the constant c is different† for different α even in homogeneous shear flows without the additional longitudinal strain. Here for the contraction (a), a crude attempt to fit (23) to the data gives

$$c \approx \begin{cases} 2 & \text{for} \quad \alpha = 1, \\ 1.2 & \text{for} \quad \alpha = 2, \\ 5.7 & \text{for} \quad \alpha = 3, \end{cases}$$

all of which are numerically greater than Rotta's value ($\simeq 1$), indicating correspondingly increased energy transfer.

For the contraction (b), the situation is somewhat more complicated. The data (joined by lines to improve clarity, with the arrows indicating the direction from upstream to the downstream of contraction) show that the component $\overline{u_1^2}$ initially starts out from being the 'donor' and $\overline{u_3^2}$ the 'receiver' of turbulent energy, but eventually reverse their respective roles, while $\overline{u_2^2}$ remains the 'receiver' all the time. There is in fact a region over which the tendency towards equipartition does not hold. Clearly, Rotta's model cannot be stretched to strained turbulence except sometimes qualitatively as in contraction (a).

For the Launder *et al.* model, we can similarly combine (23) with the diagonal version of (22) to write

$$\frac{1}{\epsilon}\frac{p}{\rho}\overline{\frac{\partial u_\alpha}{\partial x_\alpha}} = c\left[\left(1-\frac{3\overline{u_\alpha^2}}{\overline{q^2}}\right) - c'(\mathscr{P}_{\alpha\alpha} - \tfrac{2}{3}\mathscr{P})\right], \quad c' = \frac{\gamma}{c}. \tag{25}$$

The quantity within the square brackets can be plotted for various values of c' and the best value chosen for which all the data lie on a straight line; the slope of such a line gives c. Doing this, we get (see figure 14) the best combination of constants for case (a) as:

$$c_1 = 3.3, \quad \gamma = 0.53. \tag{26}$$

The values of c_1 and γ as determined here are not very different from 3.0 and 0.6 chosen by Launder *et al.* (see also Gibson & Launder 1978; Gibson & Rodi 1981. Gibson & Launder recommend a slightly higher value of 3.6 for c_1). For contraction (b), however, no combination of c_1 and γ is satisfactory. This is not surprising since, as had been shown by Leslie (1980), the basis of the Launder *et al.* model is not necessarily complete. But, this should not detract from the the fact that it appears to work reasonably at least in the case of relatively mild strains. (Similar assessments of the Daly–Harlow was also made. Detailed results are not given here but it is enough to say that its performance for the contraction (a) was marginally less satisfactory than the Launder *et al.* model; the best combination of the constants a and b was 2.8 and 1.2 respectively. No combination of these constants was satisfactory for contraction (b).)

It is useful to make one further comment regarding the Launder *et al.* model. For the much used eddy-viscosity model

$$-\overline{u_1 u_2} = \phi\left(\frac{\overline{q^2}}{2}\right)^2 \frac{1}{\epsilon}\frac{\partial U_1}{\partial x_2}, \tag{27}$$

† For the pressure–rate-of-strain terms to drop out of the turbulent-energy equation, it is, however, necessary that the value of c must be independent of α. Otherwise, it implies an artificial relationship among different values of c and the turbulent intensities. Rotta's model then will not retain its physically simple interpretation.

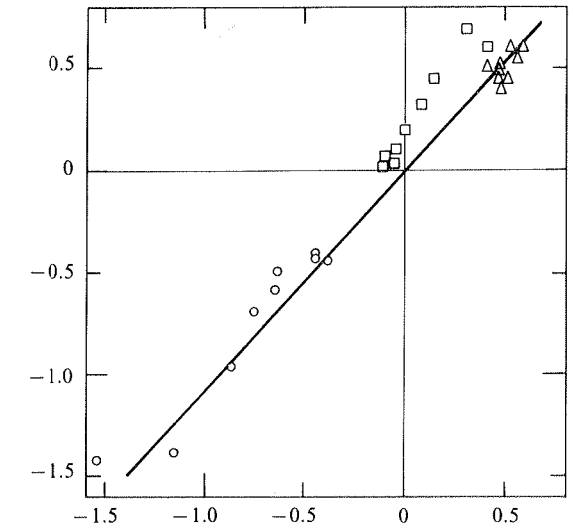

FIGURE 14. Test for the Launder–Reece–Rodi model. Ordinate and symbols as in figure 13. Abscissa are the quantities within square brackets in (26), with $\gamma = 0.53$. The slope of the line gives $c_1 = 3.3$.

using a typical experimental value of about 2 for the ratio $-\overline{u_1 u_2}(\partial U_1/\partial x_2)/\epsilon$, one obtains $\phi \simeq 0.052$. The model of Launder *et al.*, on the other hand, assumes

$$\phi = \frac{1-\gamma}{c_1}\frac{\overline{u_2^2}}{\frac{1}{2}\overline{q^2}},$$

which, with the present values of $c_1 = 3.3$, $\gamma = 0.53$ and $\overline{u_2^2}/\frac{1}{2}\overline{q^2} \approx 0.40$ (see figure 8), gives $\phi \simeq 0.057$, quite close to 0.052 above.

6. Conclusions

A uniformly sheared turbulent flow with approximate transverse homogeneity remains so at all stages of its development through a two-dimensional contraction; in fact, small deviations from homogeneity observed upstream of contraction become much less visible towards the end of contraction. The mean-flow development can be predicted adequately by the Bernoulli equation. The turbulence field, however, is not in structural equilibrium through the contraction, as indicated by the continued variation of the K parameters.

It is interesting to note that simple irrotational rapid-distortion calculations (or their variations) can be used to 'predict' the evolution of turbulent stresses for some distance downstream, although not for larger distances. That shear rapid-distortion calculations are not as successful in predicting the evolution of turbulence stresses, even though the shear strain is as rapid as, or marginally more rapid than, the longitudinal strain suggests strongly that turbulence structure responds more readily to an additional strain, and is consistent with other observations that an extra strain (be it curvature, lateral convergence or divergence) has a more dramatic effect on turbulence structure than its magnitude suggests. This fact can only emphasize the value and usefulness in the context of real flows of theories of rapid-distortion for pure strain – be it irrotational (e.g. Hunt 1977), or plane shear (e.g. Townsend 1976). This also emphasizes the importance of experiments such as those devised by Gence & Mathieu (1979) on successive distortion.

Rotta's hypothesis for the intercomponent energy exchange seems qualitatively correct (with the uncomfortable provision that the numerical constant used in (23) be different for different energy components) for the contraction (*a*) with milder acceleration, but not for contraction (*b*) with a somewhat stronger acceleration. It is uncertain that the more complex models such as those due to Daly–Harlow and Launder *et al.* are general enough (in the sense that they turn out to be inadequate in the case of the stronger contraction), but for situations typified by the contraction (*a*), these models, in particular that of Launder *et al.*, adequately describe the behaviour of the pressure–rate-of-strain terms. It is especially encouraging to note that the constants used in the model of Launder *et al.* correspond closely to those deduced from the present measurements.

I am indebted to Professor S. Corrsin for an opportunity for making these measurements in his laboratory and for several tactful lines of reminder that the manuscript is long overdue. My thanks go to Dr M. R. Maxey and a referee for their several useful comments. This work was largely supported by Grant NSG 2303 from the NASA Ames Research Centre.

Appendix: Structural equilibrium in homogeneous plane shear flows

Townsend (1976) suggested that the structural equilibrium characteristic of a given shear flow is essentially due to the finite straining effect of the mean shear on a (hypothetical) initially isotropic structureless turbulence, and the turbulence K parameters in equilibrium shear flows can be uniquely characterized by the so-called total strain. Total strain is typically the product of the finite rate of strain imposed by the mean velocity gradient and the lifetime of the large eddy. A test of the hypothesis is best made in homogeneous shear flows. Townsend (1976) did briefly examine this question in one such flow (due to Rose 1966) which had not attained energy equilibrium (e.g. the Taylor microscale was continuously increasing with x_1); clearly the question of structural equilibrium in the absence of energy equilibrium is questionable. It thus seemed worthwhile examining the ideas in other homogeneous plane shear flows that have become available since Rose's earlier experiment (Champagne *et al.* 1970; Mulhearn & Luxton 1970, 1975; Harris *et al.* 1977, and parts of the present measurements). This appendix is largely devoted to a combined study of these flows in the context of total strain as the key correlating parameter for determining the structural equilibrium of turbulence.

Townsend used the same concept also to include inhomogeneous shear flows, and achieved some success in predicting the general characteristics of the various two-point double velocity correlation functions over separation distances characteristic of eddies which are not too small. We shall also briefly examine the hypothesis as applied also to inhomogeneous shear flows, but some *a priori* comments must be made. In an inhomogeneous shear flow, eddies will have undergone a whole range of strain histories whereas in the rapid-distortion context one is using an effective average value of the parameter β. The reason that one considers an exercise such as this at all is the hope that the concept of an 'average eddy' undergoing an 'average strain history' may be adequate for discussing certain 'average properties'.

A 1. *Total strain*

Although the mean shear acts indefinitely, the total strain that the turbulence eddies experience is finite because of their finite lifetime. The obvious definition of

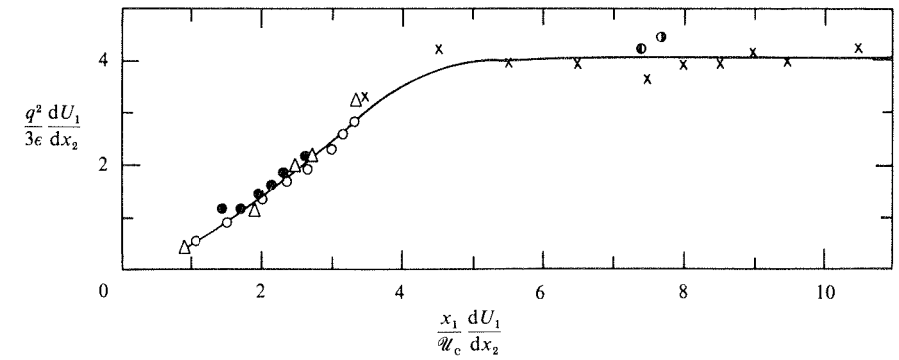

FIGURE A 1. The total strain T as a function of the parameter $(x_1/\mathscr{U}_c)\,(dU_1/dx_2)$ in homogeneous plane shear flows. ●, Rose (1966); ○, Champagne *et al.* (1971); △, Mulhearn & Luxton (1975); ×, HGC (1977); ◑, ◐ are from present experiments just upstream of contraction.

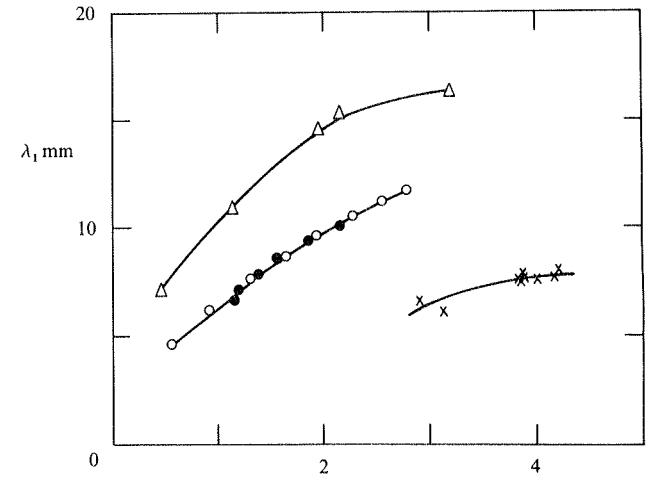

FIGURE A 2. The Taylor microscale λ_1 as a function of the total strain T. Symbols as in figure A 1.

total strain is that it is the product of the mean shear rate and the lifetime of the large eddy ($\sim \overline{q^2}/\epsilon$). We have here used the quantity

$$\beta = (\overline{q^2}/3\epsilon)\,\frac{\partial U_1}{\partial x_2}$$

in the notation of the text to represent the total strain. In the literature cited above, $(x_1/\mathscr{U}_c)\,(dU_1/dx_2)$ has been called total strain, but this is clearly not adequate because of its continual increase with x_1.

Figure A 1 shows how the total strain β evolves in the homogeneous plane shear flows under consideration. All the data collapse on a single curve. In the flows due to Rose, Mulhearn & Luxton, and Champagne *et al.* the total strain was continually increasing with x_1 and, not surprisingly, the flows did not attain their asymptotic state. On the other hand, in the HGC flow, β was a constant ($\simeq 4$) for $(x_1/\mathscr{U}_c)\,(dU_1/dx_2) \gtrsim 5$; the total strain being constant in this region, it can be expected that the structure of turbulence in the flow does not evolve any further.

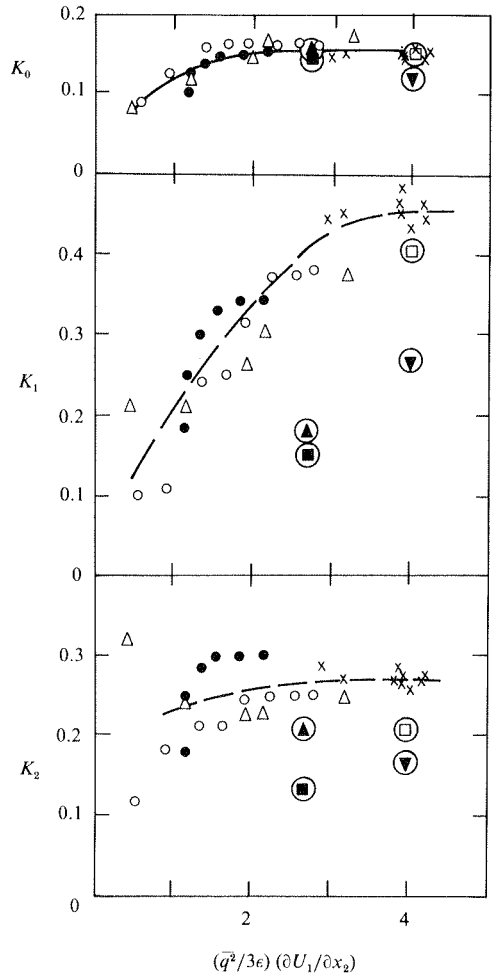

FIGURE A 3. The structural parameters K_0, K_1 and K_2 as functions of T. Symbols as in figure A 1. Additional symbols are for plane inhomogeneous shear flows: □, boundary layer (Klebanoff 1955); ■, Wake (Townsend 1956); ▲, jet (Bradbury 1965); ▼, mixing layer (Wygnanski & Fiedler 1971). For visibility they are enclosed in bigger circles.

A 2. *Energy equilibrium*

Figure A 2 shows the variation of the Taylor microscale λ_1 defined by

$$\lambda_1 = \frac{\sqrt{2}\,u_1'}{(\partial u_1/\partial x_1)'}$$

for the several flows under consideration here. In the flows of Rose and Champagne *et al.* the microscale is increasing continuously; in the Mulhearn & Luxton flow in which the total strain reaches a somewhat higher value than in the other two, λ_1 shows signs of settling down. In the HGC flow, the microscale does not grow except perhaps initially, indicating that the energy equilibrium has been reached in the flow. These observations are of course consistent with the fact that the total strain in all flows except the HGC flow are increasing with x_1.

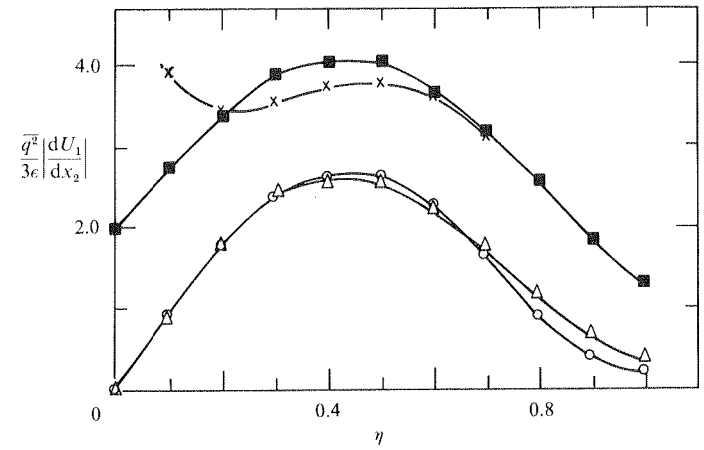

FIGURE A 4. The total strain T for the inhomogeneous plane shear flows: X, boundary layer (Klebanoff 1955), $\eta = x_2/\delta$ where δ is the boundary-layer thickness at 99.5% of the free-stream velocity; ○, Wake (Townsend 1956), $\eta = 2x_2/(x_1 d)^{\frac{1}{2}}$, where x_1 is measured from virtual origin and d is the cylinder diameter; △, jet (Bradbury 1965), $\eta = x_2/\delta_{\frac{1}{2}}$, where $\delta_{\frac{1}{2}}$ is the half-velocity thickness; ■, mixing layer (Wygnanski & Fiedler 1970), $\eta = 5(x_2/x_1 + 0.1)$, where x_2 is measured from the lip of the nozzle.

A 3. *Structural equilibrium*

In figure A 3, the structural parameters K_0, K_1 and K_2 (see (2)) are plotted as functions of β. All the data on K_0 show an increase with β for $\beta \lesssim 2$, and seem to settle down to a common constant of about 0.16 for larger β. The general pattern is the same also for K_1, which seems to settle down, for $\beta \gtrsim 4$, to a constant of about 0.45. However, for smaller β, the data from different experiments do not overlap, and show a substantial variation from one to another. This non-uniqueness for small β is even more pronounced for the parameter K_2 for which different experiments approach a constant of about 0.27 through essentially different routes. The Mulhearn & Luxton data and the Rose data, for example, have opposing trends for $\beta \lesssim 1.5$. A possible explanation for this non-uniqueness is that $\mathrm{d}\beta/\mathrm{d}t$ may also be important in developing flow.

The general conclusion appears to be that structural equilibrium may prevail for $\beta \gtrsim 4$, but not for smaller β. This is consistent with the earlier findings about energy equilibrium (see figure A 2).

In order to examine (in the spirit mentioned above) whether the structural equilibrium in inhomogeneous shear flows resembles that in homogeneous plane shear flows having the same β, we evaluated the total strain β for several standard inhomogeneous shear flows as well. The total strain β is now a function of the transverse distance (the direction of inhomogeneity), but characteristic values of total strain can nevertheless be defined. Figure A 4 shows the situation for several plane flows such as a wake, a jet, a mixing layer and a boundary layer. There is no substantial region over which β is a constant but, for wakes, jets and mixing layers, the peak is fairly flat so that these peak values can be chosen as the characteristic values. For the boundary layer,† β does not vary a great deal over some region, and the corresponding value (say near $\eta \simeq 0.4$) can be used as its characteristic value.

The structural parameters for these flows, evaluated in the regions corresponding

† Because of the energy equilibrium prevailing quite close to the wall, β must be a constant to a much better approximation there.

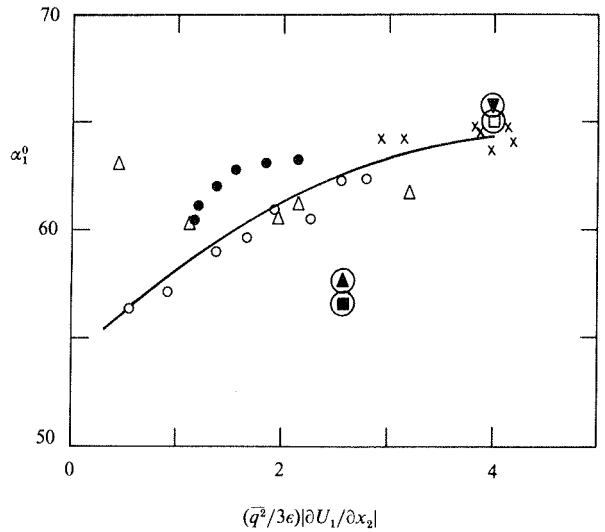

FIGURE A 5. The major angle of the principal stresses as a function of T. All symbols as in figure A 3.

roughly to the choice of the characteristic β, are also shown in figure A 3. It is clear that, except perhaps for the boundary layer, the turbulence structure is substantially different from that in the plane shear flows. It thus seems possible that other eddy structures not covered by the rapid distortion conditions will play an important role in these shear flows.

Finally, figure A 5 shows the major principal angle α_1 defined as the larger of the two angles,

$$\tfrac{1}{2}\tan^{-1}\left(\frac{-2\overline{u_1 u_2}}{\overline{u_1^2}-\overline{u_2^2}}\right),$$

plotted in the case of both homogeneous and inhomogeneous plane shear flows. For the homogeneous flows, the angle tends to asymptote to a constant for $\beta \gtrsim 4$, consistent with earlier findings. For smaller total strains, α_1 cannot be characterized by a single total strain parameter such as β. Again, not all inhomogeneous shear flows agree with the general trend. The parallel between the homogeneous and inhomogeneous shear flows is at best rather partial.

REFERENCES

BATCHELOR, G. K. & PROUDMAN, I. 1954 *Q. J. Mech. Appl. Maths* **7**, 83.

BRADBURY, L. J. S. 1965 *J. Fluid Mech.* **23**, 31.

CHAMPAGNE, F. H., SLEICHER, C. A. & WEHRMANN, O. H. 1967 *J. Fluid Mech.* **28**, 153.

CHAMPAGNE, F. H., HARRIS, V. G. & CORRSIN, S. 1970 *J. Fluid Mech.* **41**, 81.

CHOU, P. Y. 1945 *Q. Appl. Maths* **3**, 38.

DALY, B. J. & HARLOW, F. H. 1970 *Phys. Fluids* **13**, 2634.

DONALDSON, C. 1971 In *Proc. AGARD Conf. on Turbulent Shear Flows, London*, paper B-1.

FEIEREISEN, W. J., SHIRANI, E., FERZIGER, J. H. & REYNOLDS, W. C. 1981 In *Proc. Third Symp. on Turbulent Shear Flows, Davis, California*, p. 19.31.

GENCE, J. N. & MATHIEU, J. 1979 *J. Fluid Mech.* **93**, 501.

GIBSON, M. M. & LAUNDER, B. E. 1978 *J. Fluid Mech.* **86**, 491.

GIBSON, M. M. & RODI, W. 1981 *J. Fluid Mech.* **103**, 161.

HANJALIC, K. & LAUNDER, B. E. 1972 *J. Fluid Mech.* **52**, 609.

HARRIS, V. G., GRAHAM, J. A. H. & CORRSIN, S. 1977 *J. Fluid Mech.* **81**, 657.

HUNT, J. C. R. 1973 *J. Fluid Mech.* **61**, 625.

HUNT, J. C. R. 1977 *Thirteenth Biennial Fluid Dynamics Symp. Advanced Problems and Methods in Fluid Dynamics, Poland.*

KEFFER, J. F., KAWALL, J. G., HUNT, J. C. R. & MAXEY, M. R. 1978 *J. Fluid Mech.* **86**, 465.

KLEBANOFF, P. S. 1955 *N.A.C.A. Tech. Rep.* 1292.

LAUNDER, B. E., REECE, G. J. & RODI, W. 1975 *J. Fluid Mech.* **68**, 537.

LESLIE, D. C. 1980 *J. Fluid Mech.* **98**, 435.

LUMLEY, J. L. 1978 *Adv. Appl. Mech.* **18**, 124.

LUMLEY, J. L. & KHAJEH-NOURI, B. 1974 *Adv. Geophys.* **18A**, 169.

MAXEY, M. R. 1982 *J. Fluid Mech.* **124**, 261.

MULHEARN, P. J. & LUXTON, R. E. 1970 *Dept Mech. Engng Univ. Sydney Rep.* F-19.

MULHEARN, P. J. & LUXTON, R. E. 1975 *J. Fluid Mech.* **68**, 577.

NARASIMHA, R. & SREENIVASAN, K. R. 1973 *J. Fluid Mech.* **61**, 417.

PEARSON, J. R. A. 1959 *J. Fluid Mech.* **5**, 274.

PHILLIPS, O. M. 1955 *Proc. Camb. Phil. Soc.* **51**, 220.

PRABHU, A., NARASIMHA, R. & SREENIVASAN, K. R. 1974 *Adv. Geophys.* **18B**, 317.

REYNOLDS, W. C. 1976 *Ann. Rev. Fluid Mech.* **8**, 183.

RIBNER, H. S. & TUCKER, M. 1953 *NACA Tech. Rep.* 1113.

ROSE, W. G. 1966 *J. Fluid Mech.* **25**, 97.

ROTTA, J. C. 1951 *Z. Phys.* **129**, 547.

ROTTA, J. C. 1962 *Prog. Aero. Sci.* **2**, 1.

SREENIVASAN, K. R. & NARASIMHA, R. 1978 *J. Fluid Mech.* **84**, 497.

SREENIVASAN, K. R., ANTONIA, R. A. & DANH, H. Q. 1977 *Phys. Fluids* **20**, 1238.

TAVOULARIS, S. & CORRSIN, S. 1981 *J. Fluid Mech.* **104**, 311.

TOWNSEND, A. A. 1954 *Q. J. Mech. Appl. Maths* **7**, 104.

TOWNSEND, A. A. 1956 *The Structure of Turbulent Shear Flow.* Cambridge University Press.

TOWNSEND, A. A. 1976 *The Structure of Turbulent Shear Flow.* 2nd edn. Cambridge University Press.

TOWNSEND, A. A. 1980 *J. Fluid Mech.* **98**, 171.

TUCKER, H. J. & REYNOLDS, A. J. 1968 *J. Fluid Mech.* **32**, 657.

UBEROI, M. S. 1957 *J. Appl. Phys.* **28**, 1165.

WYGNANSKI, I. & FIEDLER, H. E. 1970 *J. Fluid Mech.* **41**, 327.